Li *et al. Bioresour. Bioprocess.* (2015) 2:44
DOI 10.1186/s40643-015-0074-4

Bioresources and Bioprocessing
a SpringerOpen Journal

RESEARCH

Open Access

Identification of a new thermostable and alkali-tolerant *α*-carbonic anhydrase from *Lactobacillus delbrueckii* as a biocatalyst for CO_2 biomineralization

Chun-Xiu Li[1,2†], Xiao-Chen Jiang[1†], Yong-Juan Qiu[1,2] and Jian-He Xu[1,2*]

Abstract

Background: Carbonic anhydrase (CA, EC 4.2.1.1), an ancient enzyme and the fastest among many enzymes, is a useful biocatalyst for carbon capture use and storage (CCUS). The use of alkaline buffers and high temperatures are favorable for biomineralization. Hence, the stability of CA under such harsh conditions is extremely important for its practical application.

Methods and results: Herein, we report a new thermostable and alkaline-tolerant α-CA (designated as *Ld*CA), with only 26 % identity to bovine CA (BCA), which was identified by genome mining from *Lactobacillus delbrueckii* CGMCC 8137. It was overexpressed in *Escherichia coli* in a soluble form and purified to electrophoretic homogeneity by His-Trap affinity chromatography. The dimer protein had a subunit molecular weight of 23.8 kDa and showed extremely high stability at pH 6.0–11.0 and 30–60 °C. Its activity was maintained even after incubation at 90 °C for 15 min. The half-lives of the enzyme measured at 30, 40, and 50 °C were 630, 370, and 177 h, respectively. At pH 9.0, 10.0, and 11.0, its half-lives were 105, 65, and 41 min, respectively. *Ld*CA was applied at 50 °C to accelerate the formation of calcium carbonate in a vaterite phase.

Conclusions: In summary, a new CA with high thermal and alkaline stability was identified from a general bacterium, demonstrating an effective strategy for discovering new and useful biocatalysts.

Keywords: *Lactobacillus delbrueckii*, α-Carbonic anhydrase, Stability, Biomineralization

Background

With the development of modern industry, increases in the atmospheric concentrations of CO_2, which is one of the main greenhouse gases, have led to several undesirable consequences such as global warming and associated changes (Hewett-Emmett and Tashian 1996). To this effect, various solutions have been proposed and applied, not only to reduce the concentration of CO_2, but also to recover CO_2 for reuse under the carbon capture use and storage (CCUS) scheme. The critical and rate-limiting step of these processes is the hydration of CO_2, with a reaction constant of 6.2×10^{-3} s at 25 °C (Sullivan et al. 1993). Therefore, it is necessary to explore a new method to accelerate this reaction.

A series of physical and chemical technologies for speeding up CO_2 hydration have been reported and received considerable attention over the last decade (Abu-Khader 2006). However, transformation processes using inorganic catalysts and alkaline media are costly, poisonous, and tedious. Contrarily, similar processes catalyzed by enzymes are considerably cheaper, more environmentally friendly, and energy efficient (Alvizo et al. 2014). Thus, bio-based capture is a very important and promising alternative to consider in the future.

*Correspondence: jianhexu@ecust.edu.cn
†Chun-Xiu Li and Xiao-Chen Jiang contributed equally to this study
[1] Laboratory of Biocatalysis and Synthetic Biotechnology, State Key Laboratory of Bioreactor Engineering, East China University of Science and Technology, Shanghai, 200237, China
Full list of author information is available at the end of the article

Carbonic anhydrase (CA, EC 4.2.1.1), an ancient enzyme, is known as the fastest enzyme with a maximal k_{cat} of 10^6 s^{-1}. It is a zinc metalloenzyme that catalyzes the interconversion between CO_2 and HCO_3^- (Supuran and De Simone 2015), and is undoubtedly the most suitable and direct catalyst for CCUS (Sathaye et al. 2006). The enzyme was first discovered in red blood cells and subsequently identified in most organisms including animals, plants, archaebacteria, and eubacteria (Smith and Ferry 2000). Some CAs have been isolated and characterized from different species. The enzymes exist in five distinct classes (α, β, γ, δ, and ε); the first three classes of enzymes are found in almost all prokaryotes, undertaking important physiological functions such as CO_2 and ion transport, and CO_2/bicarbonate balance required for biosynthetic reactions (Smith et al. 1999).

Additionally, CA is useful for in vitro processes. Among several carbon capture and storage (CCS) technologies, biotechnology using CA for biomimetic $CaCO_3$ mineralization holds much promise because it is viable and environmentally benign (Liu et al. 2005). An integrated system was developed, whereby CA was used to accelerate the hydration of CO_2 (Bond et al. 2001). The feasibility of using CA as a catalyst for CO_2 hydration and its precipitation to calcium carbonate was demonstrated (Liu et al. 2005; Mirjafari et al. 2007). At higher pH, two phases of $CaCO_3$ (calcite and vaterite) were observed using X-ray diffraction (XRD) and scanning electron microscopy (SEM) (Favre et al. 2009). Conversely, at pH values below 8.5, very few CO_3^{2-} ions were detected and little precipitation was observed (Jo et al. 2013).

Undoubtedly, thermostability significantly affects the application of CA in CCUS processes. Most thermostable CAs were identified in archaebacteria such as *Mt*CA from *Methanobacterium thermoautotrophicum* (Smith and Ferry 1999). Only a few brief studies have been reported on methods using CAs to facilitate CO_2 adsorption and sequestration, and the results were unsatisfactory owing to the high costs and lack of stability.

Several methods have been proposed to overcome the problems of long operation times and low stability across a wide range of pH values and temperatures. For example, BCA was immobilized in three different matrices, i.e., acrylamide, alginate, and chitosan–alginate that improved CA stability at elevated temperatures (Bond et al. 2001). Additionally, CA from *Neisseria gonorrhoeae* (*ng*CA) was highly expressed in the periplasm of *Escherichia coli* in a soluble form (Jo et al. 2013). However, such a process increased the cost of CA and was difficult to scale up to an industrial level. Therefore, a new CA with high stability and activity is still highly desirable for CO_2 hydration.

In this work, a new and highly stable CA was identified from *Lactobacillus delbrueckii* CGMCC 8137. It is the first thermostable α-CA cloned from this genus, and displayed a relatively high activity even following incubation at 90 °C for 15 min. Owing to its excellent thermal and alkaline stability, *Ld*CA appears to be promising for application in CCUS. Herein, as merely 1 mg of protein (cell free extract) was added to the reaction system, as much as 183 mg of $CaCO_3$ was yielded at 50 °C within 5 min. The crystallographic nature and crystal shape of the resulting solid were determined by XRD and SEM.

Methods

Bacterial strains and vectors

Escherichia coli DH 5α and *E. coli* BL21 (DE3), routinely grown in Luria–Bertani (LB) medium, were used as the cloning and expression hosts, respectively (Du et al. 2014). Kanamycin (50 μg ml^{-1}) was used for the selection of recombinant strains in *E. coli*. *Lactobacillus delbrueckii* was obtained from China General Microbiological Cultures Center, with an accession number of CGMCC 8137. Other strains used in this study are listed in Additional file 1: Table S1. Cells were cultured as described previously (Qian et al. 2011). Vector pET-28a (+) for heterogeneous expression studies (Chen et al. 2015) was obtained from Novagen (Shanghai, China).

Gene identification, cloning, and construction of expression plasmids

Homologous protein sequences of BCA were collected from NCBI protein sequence database using pBLAST search. Sequences were chosen with identities under 40 %. The genomic DNA of different microorganisms was extracted and purified using the TIANamp Bacteria DNA Kit from Tiangen (Shanghai, China).

PCR reaction conditions were as follows: 95 °C for 5 min, followed by 30 cycles of 94 °C for 1 min, 55 °C for 30 s and 72 °C for 1 min, and finally 72 °C for 10 min. The restriction sites and the oligonucleotides used as forward and reverse primers are listed in Additional file 2: Table S2. All the homologous genes were subcloned into expression vector pET-28a (+), and recombinant proteins were fused with C terminus His-tag. The gene insertion was verified by DNA sequencing. The constructs were transformed into *E. coli* strain BL21 (DE3) which had the gene for T7 RNA polymerase under the control of the *lac* promoter for overproduction of the CAs.

Expression and purification

The protein expression in *E. coli* BL21 (DE3) was induced by addition of 0.5 mM IPTG and 0.5 mM $ZnSO_4$ (final concentrations) and incubation at 25 or 16 °C and 180 rpm for 10 or 20 h. The induced culture broth was harvested by centrifugation (15,483×*g*), washed, and re-suspended in Tris-HCl buffer (25 mM, pH 8.3), followed

by sonication with an ultrasonic oscillator (JY92-II, Scientz Biotech Co.) for cell breakage. The supernatant and pellet fractions were separated by centrifugation at 12,000 rpm (23,225×*g*) for 10 min at 4 °C, and the protein expression was analyzed by SDS-PAGE (15 % gel).

For purification, the resultant supernatant was loaded onto a Ni-NTA column (5 ml, GE Healthcare Co.) equilibrated with buffer A (20 mM sodium phosphate buffer, pH 7.4, 500 mM NaCl, 10 mM imidazole). The proteins were eluted with an increasing gradient of imidazole from 10 to 500 mM in buffer A at a flow rate of 5 ml/min. The purity of fractions was examined by SDS-PAGE. The fractions containing the target protein were collected and dialyzed against 25 mM Tris-HCl buffer (pH 8.3) for desalting. The protein concentration and CA activity were determined by the Bradford method (Bradford 1976) with bovine serum albumin as standard and Wilbur–Anderson method (Wilbur and Anderson 1948), respectively.

Protein analysis

Gel electrophoresis was performed on 15 % SDS-polyacrylamide gel with Tris-glycine buffer system. Protein bands were visualized by staining the gel with silver stain. The apparent molecular masses were determined by gel filtration chromatography using a TSK gel 2000SWxl column (Tosoh, Japan) connected to an HPLC system equilibrated with 100 mM sodium phosphate buffer (pH 6.7) containing 0.1 M Na_2SO_4 at a flow rate of 0.4 ml/min. Protein molecular weight standards were horse heart cytochrome *c* (12.4 kDa), bovine carbonic anhydrase (29 kDa), bovine serum albumin (66 kDa), yeast alcohol dehydrogenase (150 kDa), and sweet potato β-amylase (200 kDa) from Sigma (Shanghai, China).

CO_2 hydration activity assay

The activity of *Ld*CA was detected using an accommodating electrometric method of Wilbur–Anderson (Wilbur and Anderson 1948). It was followed with some modifications. The samples were assayed at 0 °C by adding 0.1 ml of the enzyme solution or buffer to 6 ml of 25 mM Tris-HCl buffer (pH 8.3). The reaction was initiated by the addition of 4 ml ice-chilled CO_2-saturated water (pH 3.8). The activity measured in the special unit (WAU) was calculated with the equation $(t_c - t)/t$, where t is the time required for the drop in two units of pH from 8.3 to 6.3 was measured, while t_c (control) is the time required for the pH change when buffer was substituted for the test sample. Values presented were the means of three replications. The protein content was estimated using the Bradford method.

pH and temperature stability

To investigate the effect of temperature on *Ld*CA, the samples were incubated at different temperatures from 30 to 90 °C for 15 min, and then its activity was assayed at 0 °C under conditions similar to the standard assay. The tolerance of pH was assayed in different buffers (pH 3.0–11.0): sodium citrate for pH values ranging from 3.0 to 5.0, sodium phosphate for pH values ranging from 5.0 to 8.0, and Glycine–NaOH for pH values ranging from 8.0 to 11.0. The samples were incubated in different buffers for 30 min. Then, the residual activity was detected as described above. The half-lives of pH 9.0, 10.0, and 11.0 were also detected. The samples were incubated in Glycine–NaOH buffer at 30 °C. At intervals predetermined, samples of the enzyme were withdrawn, and their residual activities were measured under the standard assay condition.

Thermostability test

For the evaluation of stability, the purified *Ld*CA was pre-incubated in PBS buffer (pH 6.3) at 30, 40, 50, or 60 °C. The purified protein was diluted to a concentration of approximately 1 mg/ml. At intervals predetermined, samples of the enzyme were withdrawn, and their residual activities were measured under the standard assay condition.

Sequestration of CO_2 in $CaCO_3$

The sequestration of CO_2 was performed at high pH and temperature. CO_2 saturated solution using purified water was prepared at room temperature as described. The precipitation was detected via A_{600} using UV/vis spectrophotometer to monitor the turbidity of the reaction system. 500 µl of CO_2-saturated water was added to a reaction cuvette containing 450 µl buffer (1 M Tris, 20 mM $CaCl_2$, pH 9.0, 10.0 or 11.0) and 50 µl of samples (or Tris buffer as blank) and throughly mixed. Immediately after the cuvette was closed with a plastic cap to prevent CO_2 leakage, the reaction was performed at 30 °C. No additional Zn^{2+} was added into the reaction mixture, since the active enzyme has contained the desired metal ions in a state of complex with the protein. The natural culture medium used for fermentation of the enzyme contains a trace but enough amount of various metal ions including Zn^{2+} for cell growth and enzyme function. The required time for onset of precipitation (defined here as the first second of the time period that showed an average rate of increase more than 0.001 A_{600}/s) was recorded. Once precipitation was detected, initial slopes of absorbance curves were used to compare relative rates (Li et al. 2013).

Preparation and characterization of $CaCO_3$ solid crystals

At pH 11.0, the reaction volume was scaled up to 100 ml at 30, 40, 50 °C to prepare enough solid powder for further characterization. The cell free extract (1 mg) was added to the reaction system, in 5 min, the reaction

was terminated, and the mixture was filtered through 0.22-μm-pore membrane filters. The powder left on the membrane was dried at 65 °C until constant weight. To follow up quantitatively the generation of Ca-carbonate, the free Ca^{2+} concentration in the $CaCl_2$ solution was determined by EDTA titration (Slowinski et al. 2011).

The identities and polymorphs of the precipitates were analyzed by X-ray powder diffraction (XRD) with D/max 2550 V, using Cu α radiation operated at 40 kV and 100 mA. To determine the crystal morphology, imaging by scanning electron microscopy (SEM) was performed with S-3400N under an electrical tension of 15 kV.

Results

Expression, purification, and identification of *Ld*CA

To obtain an efficient and new carbonic anhydrase from microorganisms, homologous protein sequences of the α-CA family were collected from the NCBI protein sequence database using pBLAST. We chose 10 potential sequence encoding α-CA (Additional file 3: Table S3) and overexpressed them in *Escherichia coli* cells. During the screening process, the enzyme (*Ld*CA) from *Lactobacillus delbrueckii* CGMCC 8137, YP_618592.1, showed significant activity (110 WAU/mg). A BLAST search revealed that *Ld*CA has 26 % homology with BCA.

*Ld*CA with an *N*-terminal His-tag was purified to electrophoretic homogeneity by nickel affinity chromatography. The specific activity of the enzyme after purification reached 468 WAU/mg with a purification fold of 4.54. The purified enzyme migrated as a single band with a size of about 23.8 kDa on SDS-PAGE (Fig. 1), a molecular weight in agreement with that predicted from the gene sequence.

For analyzing the sequence of LdCA, an alignment of the amino acid sequence of some CAs belonging to the same family of *Ld*CA was done (Additional file 4: Figure S1). Compared with Human CAs I and II, and CAs from *Neisseria*, *Synechococcus*, and *Rhodopseudomona*, *Ld*CA possesses the amino acids involved in the catalytic cycle of this class of enzymes: the Zn (II) binding residues His 81, His 83, and His 97 (based on the *Ld*CA numbering). These three residues probably coordinate to the metal ion, similarly to other α-CAs investigated to date, of which some of the X-ray crystal structures have been reported (Smith and Ferry 2000). Likewise to the majority of such CAs, coordination of the zinc ion by three His residues and one H_2O ligand represents the "closed" status. Hence, the protein only exhibits activity when the H_2O is replaced by a hydroxide ion upon salt bridge formation between the H_2O and Thr158 residue. Thus, the fourth metal ligand becomes a strong nucleophile that can attack CO_2 for conversion into bicarbonate.

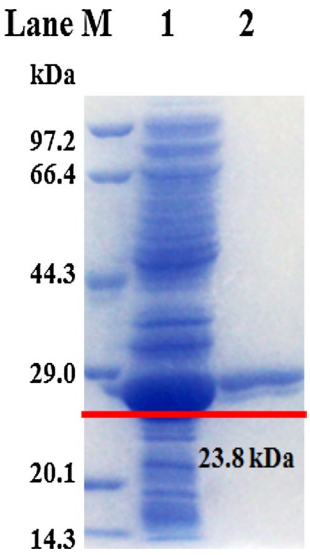

Fig. 1 SDS-PAGE of purified *Ld*CA. A 15 % gel was used for analysis. *Lane 1* Cell free extract of *Ld*CA; *Lane 2* purified *Ld*CA with a molecular weight of 23.8 kDa

pH stability and thermostability of *Ld*CA

When considering the application of CA in industry-based processes, thermostability and pH stability are key factors to examine that significantly influence the efficiency and cost of such enzyme-based CCUS technology. Enzymes that exhibit a wide pH and temperature tolerance are more suitable for CCUS. Thus, pH stability and thermostability tests were performed under the following conditions.

As shown in Fig. 2, *Ld*CA displayed stable activities under alkaline pH from 8.0 to 11.0; however, *Ld*CA was the most stable at pH 6.0. Similar results were documented for CA from *Enterobacter taylorae*. The *Bovine erythrocyte* CA displayed activity in the pH range of 6.5–7.5 and temperature range of 35–40 °C.

Stability of CA at high temperatures (40–60 °C) is required in postcombustion CCS (Lee et al. 2010; Savile and Lalonde 2011). Surprisingly, the activity of *Ld*CA was retained following incubation at 90 °C for 15 min; this represents the best result obtained to date among all the *α*-CAs cloned from bacteria. Additionally, the data were comparable with other thermostable CAs. The residual activity of *Bc*CA cloned from *Bacillus clausii* was only 8 % following incubation at 80 °C. The half-life of immobilized BCA at 60 °C is ~10 min (Bonra and Ekrem 2010).

From 30 to 60 °C, the enzyme displayed minimal activity loss and deactivated very slowly. With the increase of temperatures from 60 to 80 °C, the enzyme retained ~80 % activity at 60 °C and dropped to ~30 % activity at 80 °C. Moreover, still a 5 % residual activity

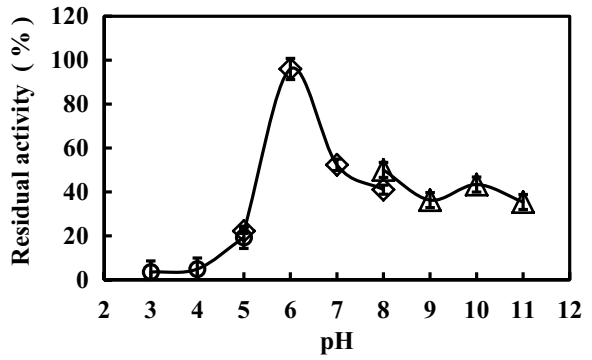

Fig. 2 The stability of pH on activity of purified *Ld*CA. The assay was carried out at 0 °C with CO_2 as a substrate, using 25 mM of different buffers for incubation: sodium citrate (*circle*); sodium phosphate (*diamond*); glycine–NaOH (*triangle*). The enzyme activity measured without any treatment was taken as 100 %

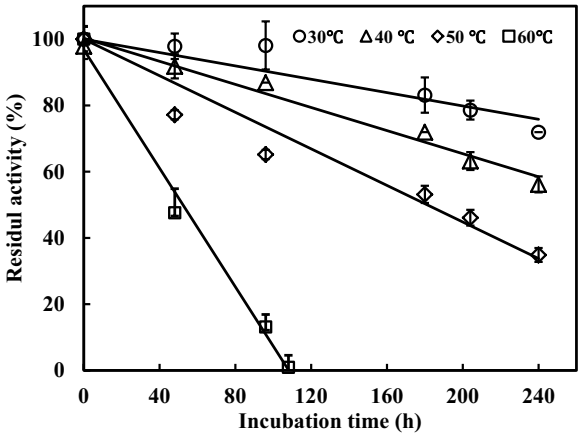

Fig. 4 Thermostability of purified *Ld*CA in a temperature range of 30–60 °C. The purified enzyme was incubated at 30 °C (*circle*), 40 °C (*diamond*), 50 °C (*triangle*), 60 °C (*cubic*) in 25 mM PBS (pH 6.0), respectively. Values are means of three parallel experiments

was observed at 90 °C (Fig. 3). The half-life of *Ld*CA was then assessed. As observed in Fig. 4, *Ld*CA preserved at least 70 % activity at 30 °C for 240 h. When the incubation temperature was further increased, the enzyme slowly lost its activity. After 100 h of reaction at 60 °C, 15 % of *Ld*CA remained active. Based on the measured deactivation rate constant (k_d), the half-lives of *Ld*CA were calculated to be 630, 370, and 177 h at 30, 40, and 50 °C, respectively. The half-lives of *Ld*CA at alkaline pHs of 9.0, 10.0, and 11.0 were 105, 65, and 41 min, respectively (Fig. 5). These results indicate that this new enzyme is very stable at high temperatures and relatively tolerant to alkaline buffers that are suitable properties for CO_2 biomineralization. To our knowledge, this is the first example of a thermostable α-CA cloned from bacteria

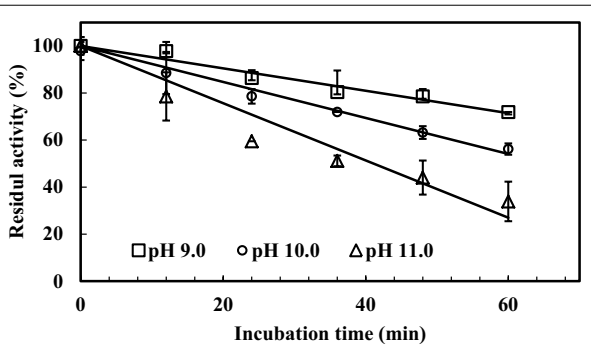

Fig. 5 Inactivation profiles of the purified *Ld*CA in a range of pH 9.0–11.0. The purified enzyme was incubated at pH 9.0 (*cubic*), pH 10.0 (*circle*), or pH 11.0 (*triangle*) in 25 mM PBS (pH 6.0), respectively, for a certain period of time. Values are means of three parallel experiments

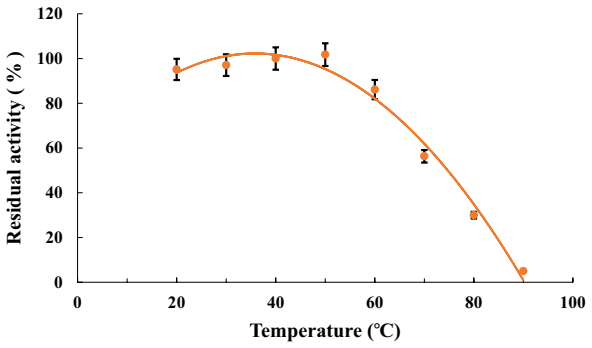

Fig. 3 The effect of temperature on activity of purified *Ld*CA. The assay was carried out at 0 °C with CO_2 as a substrate, using 25 mM Tris-HCl (pH 8.3) as buffer. Purified enzyme was preincubated at 20, 30, 40, 50, 60, 70, 80, and 90 °C for 15 min. The enzyme activity measured without any pre-treatment was taken as 100 %

Lactobacillus species. Previously, studies were focused on data mining of archaebacteria, and only one patent is available concerning thermostable CAs cloned from *Bacillus clausii* for application in CCUS (Borchert and Saunders 2010). Though the current obtained activity is not as high as that of commercial enzyme BCA, the low homology to BCA and extremely high thermostability suggest that the discovered *Ld*CA may become a useful enzyme.

Acceleration of biomineralization

To assess the ability of *Ld*CA to accelerate the biomineralization, the conversion of CO_2 into $CaCO_3$ was examined. In the presence of Ca^{2+} and CO_3^{2-}, precipitation occurred within a short time. CO_3^{2-} is produced from

HCO_3^- at a high pH (i.e., pH 11.0) because the pK_a for HCO_3^- dissociation is very high (10.3) (Lowry et al. 1951). However, CA cannot shift the equilibrium but rather accelerates the rate of this reaction. It has been reported that higher pH and temperatures are favorable for the reaction. In fact, almost no CO_3^{2-} ions exist at pH values lower than 9.0 and high temperatures will accelerate the reaction, consequently affording cooling costs reduction of the industrial gas. Furthermore, vaterite can form at high pH (Ki et al. 2013). Owing to the adequate stability of *Ld*CA, we chose pH 11.0 and 3050 °C as the reaction conditions. As observed, the reaction was completed within shorter periods at increasing temperatures (Additional file 5: Figure S2; Additional file 6: Figure S3; Additional file 7: Figure S4), and the reaction slowed down at lower pH (Additional file 8: Figure S5; Additional file 9: Figure S6). When the reaction was scaled up to 100 mL at pH 11.0, the process could also be completed within 5 min. Using a *Ld*CA catalyst load of 1 mg at 50 °C, the conversion was 91.8 % and $CaCO_3$ yield was 183 mg. In the absence of the enzyme catalyst, both the conversion and yield were lower.

To determine the crystal nature and morphology of the precipitates, XRD and SEM analyses were conducted. The morphological characteristics of the calcite and vaterite particles assessed by SEM are illustrated in Fig. 6. Vaterite was observed as spherical particles owing to its more complex packing structure. Moreover, the spherical vaterite particles were porous, unlike the slender planar calcite crystals that grew on the external surface of the vaterite particles. Based on the SEM analysis, at increasing temperatures from 30 to 50 °C, the particles featured better dispersibility properties and were more regularly shaped.

A large difference in the XRD patterns of the enzyme and enzyme-free systems was observed. In the absence of CA, the precipitate was primarily presented as the thermodynamically stable calcite phase, whereas the metastable vaterite phase dominated when the reaction was catalyzed by CA at all temperatures tested. The diffraction peaks at 2θ 29.38° and 43.90° correspond to calcite. The other main peaks at 14.18, 20.14, and 22.54 degrees were attributed to vaterite (Fig. 7). Both phases feature a hexagonal structure (Kamhi 1963; Graf 1961); however, a more complex packing was observed on the spherical surface of the vaterite crystals. Furthermore, some results have shown that calcite is the major phase obtained upon precipitation in the presence of CA (Favre et al. 2009; Li et al. 2010).

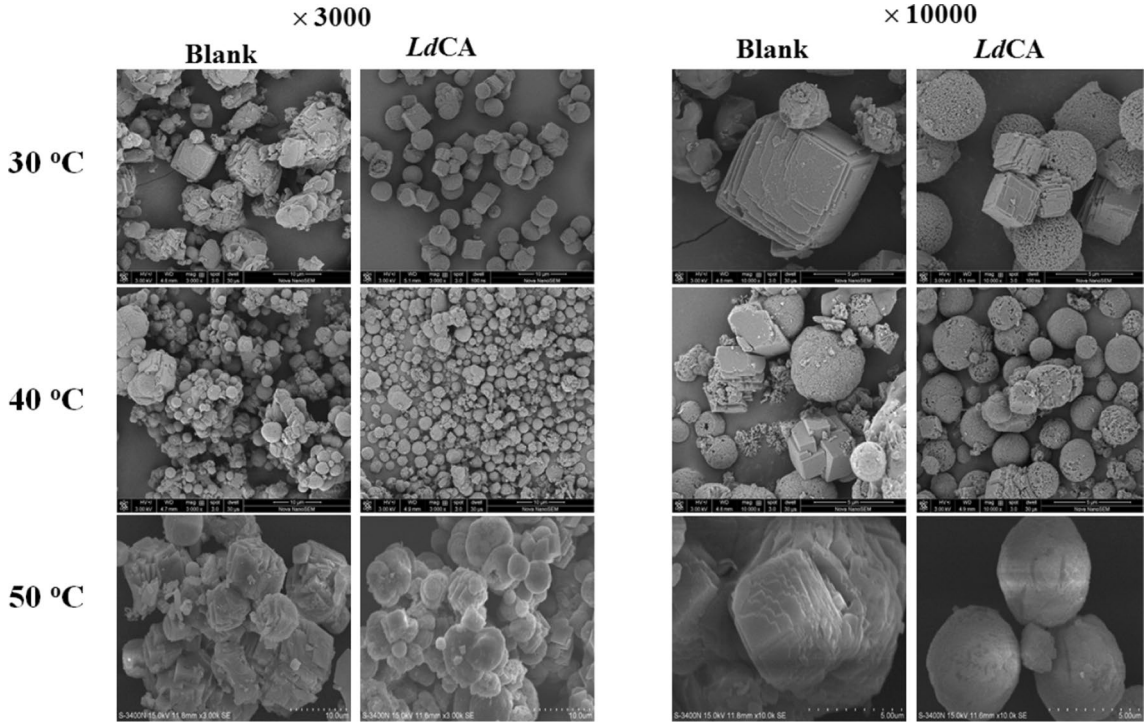

Fig. 6 SEM images of the $CaCO_3$ precipitates obtained by the different samples at 50 °C. The *scale bars* in the SEM images are 10 μm for ×3000 (*left*) and 5 μm for ×10,000 (*right*)

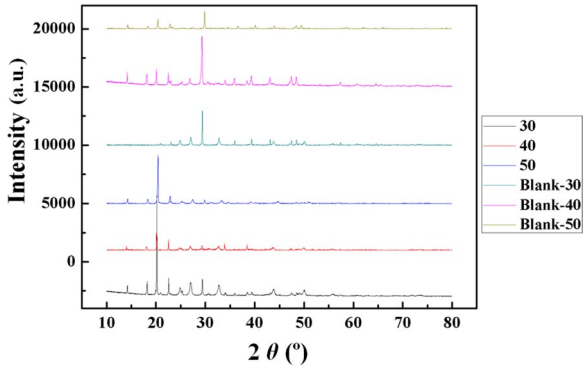

Fig. 7 XRD peaks of the $CaCO_3$ precipitates obtained by the different samples at 30, 40, and 50 °C. The *lower black line* is the biomimetically produced $CaCO_3$ and the *upper red line* is the naturally produced $CaCO_3$

Because the concentration of the protein was very low in our experiments, precipitate formation could be explained by the onset of a dissolution–reprecipitation process during aging. In this process, CA served as a catalyst to speed up the successive formation of HCO_3^- and CO_3^{2-}. Thus, the final aging process occurred at an early stage, resulting in a faster precipitate formation. So, conversion of $CaCO_3$ from the metastable vaterite phase to the thermodynamically calcite phase did not occur owing to lack of time. Additionally, the crystal nuclei that were well diffused in water did not facilitate crystal assembly.

Under the precipitation condition (pH 11.0), bicarbonate ions existed in equilibrium with carbonate ions, and in the presence of calcium ions, calcium carbonate precipitation took place (Sharma et al. 2011). Thus, CA plays an important role in the hydration reaction corresponding to calcium carbonate formation, with vaterite as the dominant form. Therefore, the application of an efficient, thermostable, and alkaline-tolerant CA will open up new avenues for cost-effective sequestration technologies of CO_2 into $CaCO_3$.

Feasibility for practical biomineralization using *Ld*CA

A few studies on biomineralization using CA from various microorganisms, such as *Pseudomonas fragi*, *Micrococcus lylae*, and *Micrococcus luteus*, have been reported (Graf 1961). Additionally, a study on constructing a whole-cell system with recombinant CA by surface display technology was also reported (Fan et al. 2011). However, all these studies resulted in relatively low enzyme activities, and the calcite was generally obtained as the major product. Hence, the use of a stable enzyme, such as *Ld*CA, that does require any pre-treatment, is crucial and highly desirable.

The first detailed investigation on the economic impact of using biologically catalyzed systems for mineralization was recently reported (Barbero et al. 2013). The study demonstrates that expenditure can be further reduced (by 4 %) if the precipitation catalyst can be used for longer times. The half-life of free *Ld*CA is about 60 times longer than the engineered system at 50 °C (Table 1). It is reasonable to expect that application of the enzyme can attain cost reduction by 16 %.

Conclusions

In this paper, we report the cloning of a thermostable CA (*Ld*CA) identified from *Lactobacillus* species and its application as enzyme catalyst for the precipitation of $CaCO_3$ to generate vaterite at 50 °C for the first time. The newly discovered enzyme shows potential for application in CCUS owing to its acceptable catalytic activity and extremely high thermostability that are desirable attributes for CO_2 biomineralization. Future work will focus on the application and immobilization of this new enzyme

Table 1 Comparison of activities among various CAs

Entry	Microorganism or system	Activity (unit)	Half-life at 50 °C (h)	Crystal form of carbonate	Conversion (50 °C/5 min)[a]	References
1	*P. fragi*	70.6 (U/mg)	4	ND	53.3	Sharma et al. (2011)
2	*M. lylae*	66.5 (U/mg)	4	ND	48.8	Sharma et al. (2011)
3	*M. luteus*	61.0 (U/mg)	8	ND	44.4	Sharma et al. (2011)
4	INP-N-CA	6.54×10^{-2} (nU/cell)	ND	Calcite and vaterite	ND	Fan et al. (2011)
5	CA2 surface-displaying yeast cells[b]	2.69×10^{-1} (nU/cell)[c]	ND	Calcite and vaterite	ND	Barbero et al. (2013)
6	periCA	1.90 (nU/cell)[c]	5	Calcite	ND	Jo et al. (2013)
7	*Ld*CA	454.0 (U/mg)	177	Vaterite	91.2	This work

[a] Conversions were determined by the weight of carbonate quantity after drying

[b] Engineering system. This is the name of the gene construct, rather than the name of the recombinant strain

[c] nU/cell represents the single-cell activity of each system

to improve its catalytic property. Improvements may be acquired via protein engineering approaches including directed evolution, rational design, or a combination of these techniques.

Additional files

Additional file 1: Table S1. Microorganisms used in this paper.

Additional file 2: Table S2. Primer sequences used to amplify the CA genes.

Additional file 3: Table S3. The results of CA gene cloning.

Additional file 4: Figure S1. CLUSTAL W alignment of carbonic anhydrase sequences from *Lactobacillus delbrueckii* (YP_618592.1), *Human* CA I (NP_001122301.1) & CA II (NP_000058.1), *Neisseria* (AAA75359.1.), *Synechococcus* (YP_400464.1) and *Rhodopseudomona* (NP_946147.1).

Additional file 5: Figure S2. Progress curve of turbidity at 30 °C. The free Ca^{2+} concentration in the $CaCl_2$ solution was determined by EDTA titration.

Additional file 6: Figure S3. Progress curve of turbidity at 40 °C. The free Ca^{2+} concentration in the $CaCl_2$ solution was determined by EDTA titration.

Additional file 7: Figure S4. Progress curve of turbidity at 50 °C. The free Ca^{2+} concentration in the $CaCl_2$ solution was determined by EDTA titration.

Additional file 8: Figure S5. Initial precipitation rates of $CaCO_3$ catalyzed by *Ld*CA at pH 11.0. The intrinsic turbidities of the cells were subtracted from the curves.

Additional file 9: Figure S6. Initial precipitation rates of $CaCO_3$ catalyzed by *Ld*CA at pH 10.0. The intrinsic turbidities of the cells were subtracted from the curves.

Authors' contributions

CXL and JHX designed the experiments and modified the manuscript. XCJ performed the experiments and drafted the manuscript. All authors read and approved the final manuscript.

Author details

[1] Laboratory of Biocatalysis and Synthetic Biotechnology, State Key Laboratory of Bioreactor Engineering, East China University of Science and Technology, Shanghai, 200237, China. [2] Shanghai Collaborative Innovation Center for Biomanufacturing, 130 Meilong Road, Shanghai 200237, China.

Acknowledgements

This work was financially supported by the Ministry of Science and Technology (2011CB710800) and the State Key Laboratory of Bioreactor Engineering, People's Republic of China.

Competing interests

The authors declare that they have no competing interests.

Received: 25 September 2015 Accepted: 19 November 2015
Published online: 30 November 2015

References

Abu-Khader MM (2006) Recent progress in CO_2 capture/sequestration: a review. Energ Sour Part A 28:1261–1279

Alvizo O, Nguyen LJ, Savile CK, Bresson JA, Lakhapatri SL, Solis EOP, Fox RJ, Broering JM, Benoit MR, Zimmerman SA, Novick SJ, Liang J, Lalonde JJ (2014) Directed evolution of an ultrastable carbonic anhydrase for highly efficient carbon capture from flue gas. Proc Natl Acad Sci USA 111:16436–16441

Barbero R, Carnelli L, Simon A, Kao A, Monforte AD, Ricco M, Bianchi D, Belcher A (2013) Engineered yeast for enhanced CO_2 mineralization. Energy Environ Sci 6:660–674

Bond GM, Stringer J, Brandvold DK, Simsek FA, Medina MG, Egeland G (2001) Development of integrated system for biomimetic CO_2 sequestration using the enzyme carbonic anhydrase. Energy Fuels 15:309–316

Bonra K, Ekrem O (2010) Thermal stability of carbonic anhydrase immobilized within polyurethane foam. AIChE J 26:1474–1480

Borchert M, Saunders P (2010) Heat-stable carbonic anhydrases and their use. US Pat 20100297723:A1

Bradford MM (1976) A rapid and sensitive method for the quantitation of microgram quantities of protein utilizing the principle of protein dye binding. Anal Chem 72:248–254

Chen J, Luo XJ, Chen Q, Pan J, Zhou J, Xu JH (2015) Marked enhancement of *Acinetobacter* sp. organophosphorus hydrolase activity by a single residue substitution Ile211Ala. Bioresour Bioprocess 2:39

Du FL, Yu HL, Xu JH, Li CX (2014) Enhanced limonene production by optimizing the expression of limonene biosynthesis and MEP pathway genes in *E. coli*. Bioresour Bioprocess 1:10

Fan LH, Liu N, Yu MR et al (2011) Cell surface display of carbonic anhydrase on *Escherichia coli* using ice nucleation protein for CO_2 sequestration. Biotechnol Bioeng 108:2853–2864

Favre N, Christ ML, Pierre AC (2009) Biocatalytic capture of CO_2 with carbonic anhydrase and its transformation into solid carbonate. J Mol Catal B Enzym 60:163–170

Graf DL (1961) Crystallographic tables for the rhombohedral carbonates. Am Miner 46:1283–1315

Hewett-Emmett D, Tashian RE (1996) Functional diversity, conservation, and convergence in the evolution of the *α*-, *β*-, and *γ*-carbonic anhydrase gene families. Mol Phylogenet Evol 5:50–77

Jo BH, Kim IG, Seo JH, Kang DG, Cha HJ (2013) Engineered *Escherichia coli* with periplasmic carbonic anhydrase as biocatalyst for CO_2 sequestration. Appl Environ Microbiol 79:6697–6705

Kamhi SR (1963) On the structure of vaterite $CaCO_3$. Acta Cristallogr 16:770–772

Ki MR, Min K, Kanth BK, Lee J, Pack SP (2013) Expression, reconstruction and characterization of codon-optimized carbonic anhydrase from *Hahella chejuensis* for CO_2 sequestration application. Bioproc Biosyst Eng 36:375–381

Lee SW, Park SB, Jeong SK, Lim KS, Lee SH, Trachtenberg MC (2010) On carbon dioxide storage based on biomineralization strategies. Micron 41:273–282

Li W, Liu L, Chen W, Yu L, Li W, Yu H (2010) Calcium carbonate precipitation and crystal morphology induced by microbial carbonic anhydrase and other biological factors. Process Biochem 238:208–214

Li W, Chen WS, Zhou PP et al (2013) Influence of initial calcium ion concentration on the precipitation and crystal morphology of calcium carbonate induced by bacterial carbonic anhydrase. Chem Eng J 218:65–72

Liu N, Bond GM, Abel A et al (2005) Biomimetic sequestration of CO_2 in carbonate form: role of produced waters and other brines. Fuel Process Technol 86:1615–1625

Lowry OH, Rosenbrough NJ, Forr AL, Randall RJ (1951) Protein measurement with Folin phenol reagent. J Biol Chem 1193:265–275

Mirjafari P, Asghari K, Mahinpey N (2007) Investigating the application of enzyme carbonic anhydrase for CO_2 sequestration purposes. Ind Eng Chem Res 46:921–926

Qian L, Liu JY, Liu JY, Yu HL, Li CX, Xu JH (2011) Fingerprint lipolytic enzymes with chromogenic *p*-nitrophenyl esters of structurally diverse carboxylic acids. J Mol Catal B Enzym 73:22–26

Sathaye J, Shukla PR, Ravindranath NH (2006) Climate change, sustainable development and India: global and national concerns. Curr Sci 3:90–95

Savile CK, Lalonde JJ (2011) Biotechnology for the acceleration of carbon dioxide capture and sequestration. Curr Opin Biotechnol 22:818–823

Sharma A, Bhattacharya A, Shrivastava A (2011) Biomimetic CO_2 sequestration using purified carbonic anhydrase from indigenous bacterial strains immobilized on biopolymeric materials. Enzyme Microb Technol 48:416–426

Slowinski EJ, Wolsey WC, Rossi RC (2011) Chemical principles in the laboratory, 10th edn. Cengage Learning, Standford

Smith KS, Ferry JG (1999) A plant type (*β*-class) carbonic anhydrase in the thermophilic methanoarchaeon *Methanobacterium thermoautotrophicum*. J Bacteriol 181:6247–6253
Smith KS, Ferry JG (2000) Prokaryotic carbonic anhydrases. FEMS Microbiol Rev 24:335–366
Smith KS, Jakubzick C, Whittam TS (1999) Carbonic anhydrase is an ancient enzyme widespread in prokaryotes. Proc Natl Acad Sci 96:15184–15189
Sullivan BP, Kirst K, Guard HE (1993) Electrical and electrocatalytical reactions of carbon dioxide, Chapter 5. Elsevier, New York, pp 118–144
Supuran CT, De Simone G (2015) Carbonic anhydrases as biocatalysts. Elsevier Science and Technology, Amsterdam
Wilbur KM, Anderson NG (1948) Electrometric and colorimetric determination of carbonic anhydrase. J Biol Chem 176:147–154